

A Matching Method for Establishing Correspondence between Satellite Radar Altimeter Data and Transponder Data Generated during Calibration

Junzhi Wan, Wei Guo, Caiyun Wang and Fei Zhao

Abstract—This letter presents a method for matching satellite radar altimeter data and transponder data generated during in situ calibration. The transponder generates a measurement error when it measures the arrival time of the altimeter’s transmitted signal and embeds the error in both the transponder’s recorded data and the altimeter’s recorded data. The second-order finite difference sequence of this error sequence can be extracted from the raw data, thus, the correspondence between two identical but mismatched second-order difference sequences can be uniquely established. The measurement error is utilized, and a data matching method that can uniquely establish the correspondence between the altimeter’s recorded data sequence and the transponder’s recorded data sequence is presented. This post-processing method does not increase the real-time signal processing workload of the transponder. Furthermore, The principles underlying this method can be used for any transponder that can adjust the response signal delay during calibration.

Index Terms—Calibration, altimeter, transponder, data matching, measurement error, correlation.

I. INTRODUCTION

A transponder is a type of ground-based auxiliary equipment for satellite radar altimetry that receives satellite altimeter signals and returns the signals to the altimeter after amplification [1]. A bent-pipe transponder receives an altimeter signal and subsequently transmits the amplified original signal [2]. Such bent-pipe transponders have already been used for in situ calibration in multiple satellite altimetry missions [3]–[6].

In 1991, a type of active transponder was proposed for the calibration of the TOPEX/Poseidon altimetry mission [7], which later became known as an active transponder for altimetry calibration (ATAC). A prototype was built, and ground field range tests were completed in November 1994. The ATAC can add arbitrary timing biases and output frequency biases

This work is part of research towards a Ph.D. being done at The Key Laboratory of Microwave Remote Sensing, Center for Space Science and Applied Research, Chinese Academy of Sciences, and University of Chinese Academy of Sciences.

Wan is with The Key Laboratory of Microwave Remote Sensing, Center for Space Science and Applied Research, Chinese Academy of Sciences, Beijing 100190, China, and University of Chinese Academy of Sciences, Beijing 100049, China (e-mail: wanjz.ac@gmail.com).

Other authors are with The Key Laboratory of Microwave Remote Sensing, Center for Space Science and Applied Research, Chinese Academy of Sciences, Beijing 100190, China (e-mail: guowei@mirslab.cn; wangcaiyun@mirslab.cn; zhaofei@mirslab.cn).

to control the delay of each response signal [2]. The ATAC records the arrival time of an altimeter signal and, after a preset time delay, reconstructs a response chirp that is the same as a chirp emitted by the altimeter. The ATAC then sends the signal back to the altimeter after amplification and optional frequency modulation. Therefore, the ATAC is a reconstructive transponder. The system structure of the ATAC is more complex than that of the bent-pipe transponder, whose internal signal runtime delay is fixed, while its new characteristics can enrich satellite radar altimeter calibration technology. However, there have been no published reports discussing the use of ATACs or other reconstructive transponders for the calibration of any satellite altimetry mission so far.

China’s marine dynamic environment satellite HY-2A was successfully launched on August 16, 2011, and a radar altimeter is one of its primary payloads [8]. To meet the absolute calibration requirements of the HY-2A altimeter, a reconstructive transponder was developed by the Key Laboratory of Microwave Remote Sensing (Mirslab), Chinese Academy of Sciences [9], [10]. A total of 20 calibrations were performed for the HY-2A altimeter using the transponder from August 9, 2012, to November 24, 2013. A number of preliminary results have been obtained by processing the preliminary data; however, a comprehensive analysis of the data requires more in-depth work. In the following text, the term “transponder” refers to the reconstructive transponder for the HY-2A altimeter calibration, and the term “altimeter” refers to the HY-2A altimeter unless stated otherwise.

During the course of a satellite pass, the transponder receives the altimeter’s transmitted signal, measures and records the time interval between the currently received signal and previously received signal, adjusts the delay of the response signal, and retransmits the reconstructed signal. Because of the limited length of the altimeter’s measurement range window, the number of recorded waveforms from the altimeter is typically less than the number of recorded waveforms from the transponder. However, the One-Receive-One-Transmit characteristic of the transponder inherently ensures a one-to-one correspondence between the altimeter’s received signal sequence and a part of the transponder’s received signal sequence.

To our knowledge, no radar altimeter calibration method that utilizes the transponder’s received signal has been publicly reported for the calibration of any satellite radar altimetry mission. Our calibration method uses both the altimeter data

and transponder data. Correspondence between the altimeter data and transponder data must be established for further transponder data uses, such as the calibration of the range and sigma naught. This problem can be described as follows: $A[m], m = 1, 2, \dots, M$ is the altimeter's recorded data sequence, and $T[n], n = 1, 2, \dots, N$ is the transponder's recorded data sequence. Suppose that $M < N$, and find a non-negative integer $k, 0 \leq k \leq N - M$ that satisfies $A[p]$ corresponds to $T[p + k], 1 \leq p \leq \min(M, N)$.

There is no existing solution, to our knowledge, to match the altimeter observations and transponder observations. In this letter, a novel approach is introduced for establishing the correspondence between the altimeter's recorded data and the transponder's recorded data. As a post-processing method, this approach utilizes the measurement error, which objectively exists in both $A[m]$ and $T[n]$, without increasing the real-time signal processing workload of the altimeter and transponder. The transponder can also adjust the delay of each response signal to embed a sequence in the altimeter's recorded data. In this case, this approach can be used, but additional real-time signal processing by the transponder is required.

II. BACKGROUND

A. Altimeter

The HY-2A radar altimeter is a pulse-compression radar, operating by the full de-ramp principle [11]. For the absolute calibration, the altimeter is switched to search mode before reaching the point of closest approach to the transponder position. In this mode, the altimeter records signal waveforms that contain the transponder's transmitted signal. The time interval between adjacent transmission operations and the time interval between the transmission and receiving operations are both fixed at certain preset values. The time interval between transmitting and receiving is sufficiently large to remove the echo signal from Earth's surface, but the transponder's signal can be sent into the altimeter range window by properly presetting the signal run-time delay.

B. Transponder

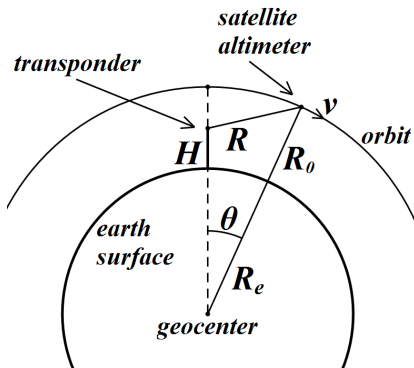


Fig. 1. Satellite/transponder positional relationship.

The dechirped altimeter signal is a single frequency base band signal, and its frequency is a function of time. The

transponder calculates the arrival time of the altimeter signal accurately using the power spectrum of the dechirped altimeter signal by real-time Fast Fourier Transformation(FFT), therefore, the quantization error introduced by the limited resolution of the FFT and other non-ideal characteristics of hardware (e.g., finite word length effects) constitute the corresponding time measurement error.

The transponder operates in the Ku-band with a 320 MHz bandwidth at a center frequency of 13.58 GHz and in the C-band with a 160 MHz bandwidth at a center frequency of 5.25 GHz based on the chirps emitted by the altimeter onboard the HY-2A. Before the satellite passes over a calibration site, the transponder receives the signal without sending a signal back. The decreasing distance between the transponder and moving satellite increases the transponder's received signal power. When the received signal power exceeds the minimum receivable power, The transponder, which is operating by the full de-ramp principle, begins to measure the arrival time of each altimeter signal in the following manner: The de-ramp operation, which is controlled by the local clock, begins at t_c when the altimeter signal is detected. t_c is an integer multiple of the clock cycle. The dechirped altimeter signal is a single frequency base band signal, and its frequency, f_{ar} , is estimated using its power spectrum derived from the real-time FFT. The frequency of the original altimeter chirp signal is a linear function of time, therefore, t_f , the time interval less than one clock cycle, is derived from $f_{ar} \cdot t_{ar}$, the sum of t_c and t_f , is the altimeter signal arrival time.

The transponder begins to send a chirp signal back, and records the time intervals between adjacent received signals after establishing precise altimeter tracking. To ensure that the response signal can be sent in the altimeter range window, the total run-time delay of each transponder signal is typically fixed at a preset value. However, the delay of each transponder signal can be adjusted in accordance with a predefined method. If the received signal power is lower than the minimum receivable power, the transponder stops sending the signal and stops recording data.

III. PRINCIPLE AND ALGORITHM

Different signal models for altimeter calibration using a transponder can be found in [2], [12]. We provide an expression based on [2]. The two-line element (TLE) data indicated that the HY-2A orbit had an eccentricity of no more than 0.00019 under normal circumstances from Jan 1, 2012 to Jan 1, 2014; thus, the circular orbit assumption is used. As shown in Fig. 1, R_e is the radius of Earth, R_0 is the distance between the altimeter and nadir point, R is the slant range between the altimeter and transponder, H is the height of the transponder relative to Earth's surface, θ is the angle between the transponder-geocenter line and altimeter-geocenter line, and v is the velocity of the satellite.

From the law of cosines, R is equal to

$$\sqrt{(R_e + R_0)^2 + (R_e + H)^2 - 2(R_0 + R_e)(R_e + H)\cos\theta}. \quad (1)$$

Using Taylor series expansions of $\cos\theta$ and $(1+x)^\alpha$, and an assumption of uniform circular motion, (1) can be rewritten

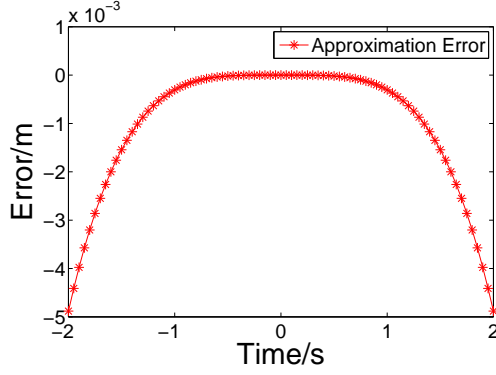


Fig. 2. Approximation error introduced by using Taylor series expansions of $\cos\theta$ and $(1+x)^\alpha$

as

$$R(t) = (R_0 - H) + \frac{(R_e + H)GM}{2(R_0 - H)(R_e + R_0)^2}t^2, \quad (2)$$

where $GM = 3.986 \times 10^{14} \text{ m}^3\text{s}^{-2}$ is a constant. R is a quadratic function of time t . Without loss of generality, (2) can be expressed as

$$R(t) = at^2 + bt + c, a \neq 0, \quad (3)$$

where a , b , and c are constants. As shown in Fig. 2, using typical values of $R_e = 6371 \text{ km}$, $R_0 = 971 \text{ km}$, $H = 55 \text{ m}$, and $t \in [-2, 2] \text{ s}$, the absolute values of the differences between the ranges derived from (1) and (2) are no more than 0.5 mm.

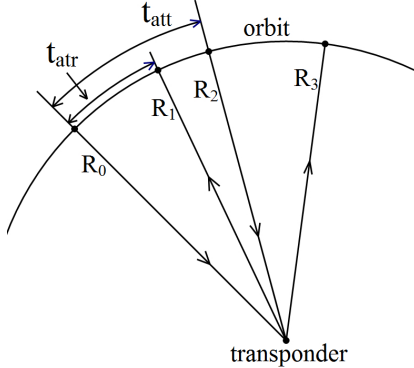


Fig. 3. Satellite/transponder transmitting/receiving relationship.

Considering measurement errors, a mathematical model for the signal transmission process between an altimeter and transponder can be established as follows. As shown in Fig. 3, R_0 and R_2 are the ranges between the altimeter and the transponder when the altimeter transmits signals, R_1 and R_3 are the ranges between the altimeter and the transponder when the altimeter receives signals, t_{att} is the time interval between adjacent altimeter transmission operations, t_{atr} is the time interval between the altimeter transmitting operation and corresponding receiving operation. Both t_{att} and t_{atr} are constants during calibration.

The altimeter transmits signals at time t_{a0} and t_{a2} , the signals reach the transponder at time t_{r0} and t_{r1} , and D_{r0} is the time interval between t_{r0} and t_{r1} . Let the sum of the

time measurement error and the instrumental noise be e . Considering the sum of altimeter's and transponder's instrumental biases B_i , atmospheric delay B_{atm} , range bias B_{ao} introduced by the frequency bias of the oscillator that provides the time reference to the altimeter, and one-way Doppler effect delay $k_1t + l_1$, let the sum of B_i and B_{atm} be B , we have

$$D_{r0} = t_{att} + \frac{(R_2 + B + k_1t_{a2} + l_1)}{C} - \frac{(R_0 + B + k_1t_{a0} + l_1)}{C} + (e_1 - e_0) + B_{ao} \quad (4)$$

where e_0 and e_1 are the samples of e at t_{r0} and t_{r1} , and C is the speed of light in vacuum.

Using (3) and (4), the transponder's recorded signal D_t can be written as

$$D_t \approx t_{att} + \frac{(2at_n + b)t_{att}}{C} + \frac{k_1t_{att}}{C} + D[e(t_n)] + B_{ao} \quad (5)$$

where $n=1,2,\dots,N$ and $D[\dots]$ is an adjacent-sample differential operator that satisfies

$$D[e(t_n)] = e(t_n) - e(t_{n-1}). \quad (6)$$

Using (3), considering B_i , B_{atm} , B_{ao} and the two-way Doppler effect delay $k_2t + l_2$, the altimeter range R_a can be written as

$$R_a = at_m^2 + bt_m + c + Ce(t_m) + B_i + 2B_{atm} + B_{ao} + k_2t_m + l_2, \quad (7)$$

where $m = 1, 2, \dots, M$.

Differentiating both sides of (7) twice and differentiating both sides of (5), we obtain

$$D^2[R_a] = 2a + CD^2[e(t_m)] \quad (8)$$

and

$$D[D_t] = \frac{2at_{att}^2}{C} + D^2[e(t_n)]. \quad (9)$$

The instrumental biases, atmospheric delays, biases introduced by the altimeter clock, and Doppler effect delays are eliminated.

The error second derivatives (ESDs) can be obtained from (8) and (9), i.e.,

$$\begin{aligned} esd_a &= \frac{1}{C}(D^2[R_a] - 2a) \\ esd_t &= D[D_t] - \frac{2at_{att}^2}{C}. \end{aligned} \quad (10)$$

Let the ESD of the instrumental noise of the altimeter be esd_{an} , the ESD of the instrumental noise of the transponder be esd_{tn} , and the ESD of the time measurement error be esd_0 , we obtain

$$\begin{aligned} esd_a &= esd_0 + esd_{an} \\ esd_t &= esd_0 + esd_{tn}. \end{aligned} \quad (11)$$

esd_{an} , esd_{tn} and esd_0 are zero mean, pairwise independent sequences. Therefore, $CR[m]$, the cross correlation sequence of esd_a and esd_t , is obtained from (11), i.e.,

$$\begin{aligned} CR[m] &= E\{esd_a[n+m]esd_t[n]\} \\ &= E\{esd_0[n+m]esd_0[n]\} \end{aligned} \quad (12)$$

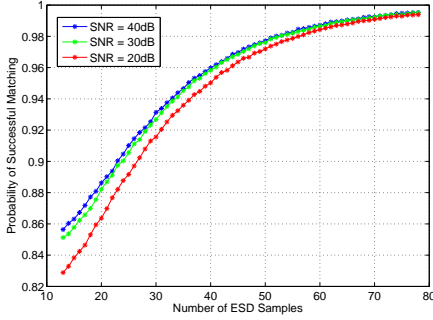


Fig. 4. Probability of Successful Matching.

Let e_0 be the time measurement error sequence, and esd_0 can be written as

$$esd_0[p] = e_0[p+2] - 2e_0[p+1] + e_0[p]. \quad (13)$$

Assuming esd_a leads the corresponding part of esd_t for k points and using (12), (13), we obtain

$$CR[m] = \begin{cases} 6\sigma_0 & m = k \\ -4\sigma_0 & m = k \pm 1 \\ \sigma_0 & m = k \pm 2 \\ 0 & m \neq k \pm 2, k \pm 1, k. \end{cases} \quad (14)$$

σ_0 is the variance of e_0 . Therefore, the cross correlation operation suppresses the influences of the instrumental noises and highlights the peak contributed by the time measurement errors of the transponder.

Let the esd_0 power to the total power of esd_{an} and esd_{tn} ratio be SNR. The relationship of probability of successful matching and the number of ESD samples under certain SNR values, which is presented in Fig. 4, is calculated by numerical simulation. The HY-2A altimeter calibration with transponder provides a SNR of 22.69dB, and corresponding probability of successful matching is 87.1%.

The algorithm is briefly presented below:

(1) Obtain the altimeter's recorded data sequence $A[m]$ for $m = 1, 2, \dots, M$ and the transponder's recorded data sequence $T[n]$ for $n = 1, 2, \dots, N$. The mathematical expressions for $A[m]$ and $T[n]$ are (7) and (5), respectively.

(2) Calculate the second-order finite difference of $A[m]$ and the first-order finite difference of $T[n]$ and obtain $esd_a[m]$ and $esd_t[n]$ defined in (10).

(3) Calculate the cross-correlation sequence of $esd_t[n]$ and $esd_a[m]$. The index corresponding to the maximum of the cross-correlation sequence is lag k .

Because reconstructive transponder records all of $D_t[n]$ and the HY-2A altimeter records $R_a[4m+1], m = 0, 1, \dots$ during calibration, the algorithm is adjusted. $D_t[4p+1], p = 0, 1, \dots$ instead of $D_t[n]$ are used in step 1, and $A[m]$ is leading the corresponding part of $T[n]$ for $4k$ points, where k is derived from step 3.

IV. RESULTS AND DISCUSSION

All examples below are from processing results of the Ku-band data of the HY-2A altimeter and the transponder. The correspondence between the altimeter data and transponder

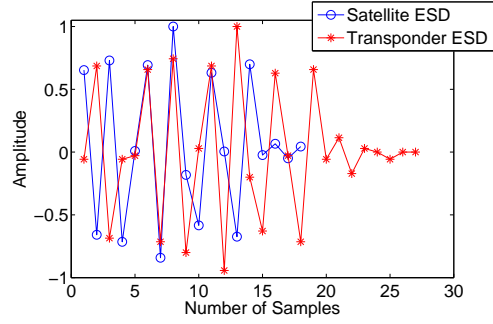


Fig. 5. Mismatched normalized satellite and transponder ESD sequences.

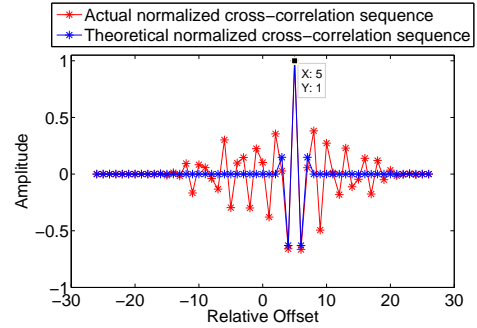


Fig. 6. Actual and theoretical normalized cross-correlation sequences of the mismatched normalized satellite and transponder ESD sequences in Fig. 6 (negative lags have no physical meaning).

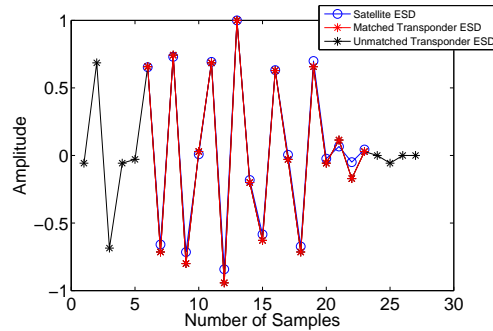


Fig. 7. Matched normalized satellite and transponder ESD sequences.

data was successfully established in 12 of the 20 calibrations that were performed. The matching method could not be implemented on the remaining failed calibrations because of a lack of altimeter-recorded waveforms. Fig. 5, Fig. 6, and Fig. 7 are from a calibration performed on January 20, 2013 in Beijing, China. Mismatched, normalized ESDs of both $A[m]$ and $T[n]$ are shown in Fig. 5. Fig. 6 presents the normalized cross-correlation sequence of the two ESDs in Fig. 5, and corresponding theoretical sequence derived from (14). The index corresponding to the maximum of the cross-correlation sequence indicates that esd_a is leading the corresponding part of esd_t for 5 points, and $A[m]$ is leading the corresponding part of $T[n]$ for 20 points. Fig. 7 presents the matched normalized altimeter ESD and the corresponding part of the transponder ESD. The mismatched part of the transponder ESD is abandoned. After successful matching, the transponder recorded data are used to compensate the

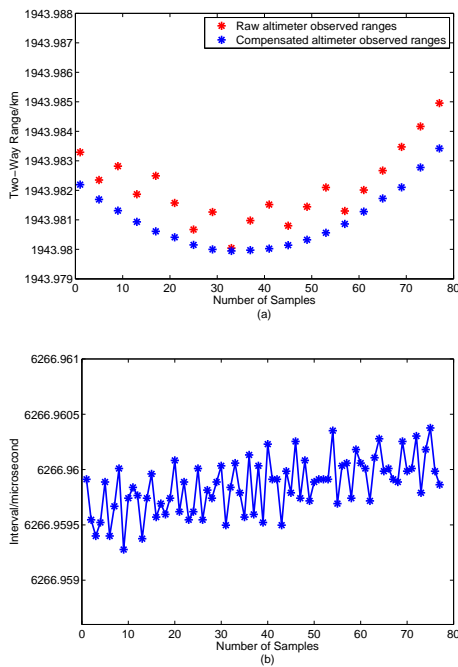


Fig. 8. (a) Raw and compensated altimeter recorded data and (b) corresponding transponder recorded data (transponder records all of $D_t[n]$ and HY-2A altimeter records $R_a[4k+1]$, $k = 0, 1, \dots$ during calibration).

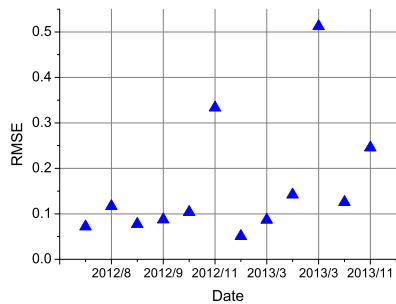


Fig. 9. RMSE between matched normalized altimeter and transponder ESDs.

fluctuations of the raw altimeter observed ranges. Fig. 8 presents raw and compensated altimeter observed ranges and transponder observed intervals.

The successful matching indicates that the altimeter ESD and the corresponding part of the transponder ESD are theoretically identical. The root-mean-square error (RMSE) is used to measure the difference between the matched altimeter and transponder normalized ESDs identified by the proposed method as shown in Fig. 9. Higher RMSE values indicate a lower confidence in the matching results.

V. CONCLUSION

As stated previously, the matching of altimeter data to transponder data is the basis for using transponder-recorded data for altimeter calibration, and the matching method introduced here provides a feasible solution to this problem. Furthermore, it should be possible for reconstructive transponders to reduce the arrival time measurement error as technology

develops further. In this case, the principle of this method would then also be applicable.

REFERENCES

- [1] P. Pesec, H. Snkel, and N. Windholz, "The use of transponders in altimetry," in *Gravity and Geoid*, ser. International Association of Geodesy Symposia, H. Snkel and I. Marson, Eds. Springer Berlin Heidelberg, 1995, vol. 113, pp. 394–400.
- [2] M. B. Mathews, "Design, testing, and performance analysis of transponders for use with satellite altimeters." Ph.D. dissertation, University of Colorado, Boulder, the USA, 1995.
- [3] E. Cristea and P. Moore, "Altimeter bias determination using two years of transponder observations," in *Proceedings of the Envisat symposium*, Apr. 2007, pp. 23–27.
- [4] W. Hausleitner, F. Moser, J.-D. Desjonqueres, F. Boy, N. Picot, J. Weingrill, S. Mertikas, and A. Daskalakis, "A new method of precise Jason-2 altimeter calibration using a microwave transponder," *Marine Geodesy*, vol. 35, no. sup1, pp. 337–362, Dec. 2012.
- [5] S. P. Mertikas, R. T. Ioannides, I. N. Tziavos, G. S. Vergos, W. Hausleitner, X. Frantzis, A. Tripolitsiotis, P. Partinevelos, and D. Andrikopoulos, "Statistical models and latest results in the determination of the absolute bias for the radar altimeters of Jason satellites using the gavdos facility," *Marine Geodesy*, vol. 33, no. sup1, pp. 114–149, Aug. 2010.
- [6] C. R. Francis and G. Ratier, "Cryosat in-flight calibration approach," ESA, Noordwijk, The Netherlands, Tech. Rep., Jan. 2005.
- [7] P. MacDoran and G. Born, "Time, frequency and space geodesy: impact on the study of climate and global change," *Proc. IEEE*, vol. 79, no. 7, pp. 1063–1069, Jul. 1991.
- [8] X. Jiang, M. Lin, J. Liu, Y. Zhang, X. Xie, H. Peng, and W. Zhou, "The HY-2 satellite and its preliminary assessment," *International Journal of Digital Earth*, vol. 5, no. 3, pp. 266–281, May. 2012.
- [9] W. Guo, X. Y. Gong, X. Y. Xu, H. G. Liu, C. D. Xu, and Y. H. Du, "A transponder system dedicating for the on-orbit calibration of china's new-generation satellite altimeter and scatterometer," in *Radar (Radar), 2011 IEEE CIE International Conference on*, vol. 1, 2011, pp. 22–25.
- [10] X. Y. Xu, W. Guo, H. G. Liu, L. W. Shi, W. M. Lin, and Y. H. Du, "Design of the interface of a calibration transponder and an altimeter / scatterometer," in *IEEE IGARSS, 2011*, pp. 953–956.
- [11] K. Xu, J. Jiang, and H. Liu, "HY-2A radar altimeter design and in flight preliminary results," in *Geoscience and Remote Sensing Symposium (IGARSS), 2013 IEEE International*, July 2013, pp. 1680–1683.
- [12] R. Powell, "Relative vertical positioning using ground-level transponders with the ERS-1 altimeter," *IEEE Trans. Geosci. Remote Sens.*, vol. GE-24, no. 3, pp. 421–425, May. 1986.